Journal of Pharmacy

Optimisation of Supercritical Fluid Extraction for Fatty Acids from Benincasa hispida Seed Oil: A Response Surface Approach

Rizal Za'im Ramli[1], Zaidul Islam Sarker[2], Hazrina Hadi[1,3]

[1]*Dermatopharmaceutics Research Group, Faculty of Pharmacy, International Islamic University of Malaysia, Jalan Sultan Ahmad Shah, Bandar Indera Mahkota, 25200, Kuantan Pahang, Malaysia.*

[2]*Food Science Program, Cooperative Research, Extension, and Education Services (CREES), Northern Marianas College P.O. Box 501250, Saipan MP 96950, USA.*

[3]*IKOP Sdn. Bhd, Jalan Sultan Ahmad Shah, 25200 Kuantan, Pahang, Malaysia.*

Abstract

Introduction: The goal of this study was the optimisation of the process parameters for the extraction of *Benincasa hispida* seed extract using the supercritical carbon dioxide. **Methods:** Response surface methodology was carried out using the design expert software with the implementation of process parameters including the temperature (40°C – 70°C), pressure (100 bar – 400 bar) and supercritical carbon dioxide flow rate (2 g/min – 10 g/min) in this study due to their significant impact towards the oil yield and the polyunsaturated fatty acids. **Results:** The optimised parameter for this supercritical fluid model is 70°C, 247 bar and 7 g/min while 0.36 bar and 40 °C has been chosen from previous studies as the optimised parameter for Soxhlet extraction. The oil yield (33% from Soxhlet extract and 9.67% from supercritical fluid extract) obtained was quite similar with previous studies, however, the polyunsaturated fatty acids obtained throughout this optimisation were much higher indicating that this study provided better output of the polyunsaturated fatty acids obtained from the seed oil. Moreover, the polyunsaturated fatty acids contents were also compared between the extract obtained from the conventional Soxhlet extraction versus novel supercritical fluid extraction techniques. **Conclusion:** The result shows the polyunsaturated fatty acids in the supercritical fluid extraction were significantly higher than the Soxhlet extraction due to the advantages and suitability of the polyunsaturated fatty acids extraction using the supercritical fluid extraction method.

Article history:

Received: 6 March 2025
Accepted: 10 July 2025
Published: 31 July 2025

Keywords:

Benincasa hispida
Supercritical fluid extraction
Response surface methodology
Optimisation
Polyunsaturated fatty acids

doi: 10.31436/jop.v5i2.392

*Corresponding author's email: hazrina@iium.edu.my

Introduction

Benincasa hispida or also known as komora (Assamese) or kushmanda (Sanskrit) is a fruit that is widely produced and consumed in the North-East India (Mondal *et al*., 2020). The fruit has proven to be beneficial to human health due to its potential for medicinal and pharmaceutical purposes. For instance, antioxidant, anti-ulcer, anti-inflammatory, anti-obesity, anti-compulsive and anti-diarrheal activities that can be exerted by *B. hispida* (Shakya *et al*., 2020). India and South-East Asian countries are the two most cultivation places for this fruit (Gade *et al*., 2020).

B. hispida is considered as a fruit vegetable which is rich in nutritional components as functional food and nutraceutical market products. Two cultivars of Kundur are grown in Malaysia, which are the round shaped and elongated. *B. hispida* is one of the Cucurbitaceae family. *B. hispida* can be characterized by its large leaves, an annual creeper and bristly hairs on its thickly covered fruit skin (Megashree *et al*., 2017).

Despite growing interest in the beneficial properties of natural plant-based oils for their nutritional and therapeutic properties, there is limited scientific data on the optimal extraction of *B. hispida*. Traditional extraction such as solvent extraction and cold pressing often results in a much lower yields and degradation of the targeted compounds (Hou et al., 2024).

Additionally, the application of modern and greener types of extraction [supercritical fluid extraction (SFE)] is preferable. Moreover, most studies related to this plant only focused more on the beneficial effect of *B. hispida* seed oil rather than the optimization process and the fatty acid contents (Muzahid et al., 2023; Boniamin et al., 2024). Therefore, the implementation of optimization process by using statistical approach (response surface methodology) is tailored to enhance the extraction efficiency and preserving the quality of the targeted active compounds.

There was one study of SFE of *B. hispida* that was done for the optimization purposes (Bimakr et al., 2013). The parameters involved in that study were pressure (150-300 bar), temperature (40-50°C) and dynamic extraction time (60-120 min) towards the oil yield using response surface methodology (RSM) for optimization. Therefore, the aim of this study was to optimize different extraction parameters of the *B. hispida* seed extract (BHSE) using RSM and to compare the polyunsaturated fatty acids (PUFAs) content between the extracts from both SFE and Soxhlet extraction (SE) and their fatty acid (FA) profile.

Materials and methods

Materials

Whole winter melons (*B. hispida*) were purchased from a local market at Kuantan, Pahang Malaysia. The fruits were chosen with similar characteristics such as the color, size and absence of surface defects. N-hexane (Merck, Germany) was used as the solvent for the SE. The supercritical fluid extractor (SFE Waters Thar, USA) with the carbon dioxide (CO_2) industrial grade (GasWORLD, Malaysia) were implemented. Besides that, sodium methoxide (Thermo Fisher Scientific, USA) and fatty acid methyl ester (FAME) standards (Sigma Aldrich, Germany) were used for gas chromatography analysis and all chemicals were purchased either in chromatography or analytical grade.

Method

Seed preparation method

The fruits were sliced, and the seeds were separated manually from the fruit. Later, the seeds were washed under running tap water. Then, the seeds were dried at 40°C in a ventilated oven for 24 hours and stored at ambient temperature in the dark container (Bimakr *et al*., 2013). Grinder mill (300 RPM) was used to grind the seeds into powder form to reduce the particle size and thus enhance the extraction efficiency (Bimakr *et al*., 2013).

Supercritical fluid extraction (SFE)

SFE was carried out using the supercritical fluid apparatus including 500 mL extraction vessel, automated back pressure regulator and CO_2 pump. ICE software was used to control the flow rate of

CO_2, extraction temperature and pressure while the extraction time was measured using the stopwatch. Samples of ground *B. hispida* seeds (10 g) and glass beads (120 g with 2.0 mm in diameter) were mixed and placed into the extraction vessel.

SFE of BHSE was performed on laboratory scale at the INHART, Gombak Malaysia. Based on Fig. 1, firstly, the liquid CO_2 released towards the cooling bath circulator to ensure that the liquid CO_2 was maintained at liquid state. Then, it was transferred using CO_2 pump to the heat exchanger to convert the liquid CO_2 into supercritical fluid. The vessel was heated up to the desired temperature while pumping the supercritical solvent phase into the vessel to reach values set by system (Bimakr *et al.*, 2011).

Then, the solvent was pumped into the extractor vessel where the supercritical stream dissolved targeted components and moved towards the fraction collector. After the pressure nearly reached the targeted set value, the extraction process starts by the automatic opening of the automated back pressure regulator (ABPR) which allows the continuous flow of solvent through the extractor while carrying the solubilized components to the separator. Lastly, the CO_2 will be released through the last valve (Rovetto and Aieta, 2017). 100-400 bars of pressure, 40-70°C of temperature and 2-10g/min flow rate were used for the extraction process. The extraction time was maintained at 90 minutes.

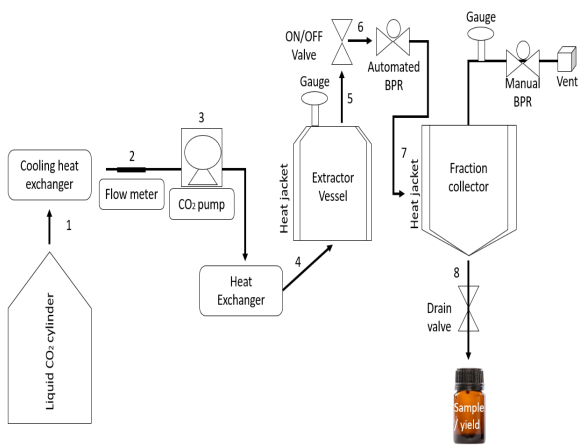

Fig. 1: General diagram for SFE

After the desired temperature and pressure have been obtained, the *B. hispida* seeds were soaked in the solvent for 30 min to equilibrate the mixture at desired pressure and temperature to enhance solvent penetration into the cellular walls and increase the oil yield (Bitwell et al., 2023). The static extraction time was applied at different desired pressure and temperature for each conducted run. During the dynamic extraction time, CO_2 carrying the released solutes will flow out of the unit and the extract was collected in the pre-weighted collection flask. The procedure was carried out in triplicate for a total of 17 runs for one complete cycle (Table 2). The extract was weighed using analytical balance and the total extractable components (TEC) were calculated using following Equation 1 (Nawaz et al., 2020):

$$\text{TEC (\%)}: \frac{\text{Weight of Extract}}{\text{Weight of Sample}} \times 100\% \qquad (1)$$

Soxhlet extraction (SE)

300 mL of n-hexane was measured and poured into the round bottom flask containing a small amount of boiling chips. The extraction process was done for a duration of 6 hours (Al-Juhaimi and Özcan, 2017). After 6 hours, the solvent containing the extracts was filtered using Whatman filter paper. Then, it was evaporated using the rotary evaporator with 360 mbar pressure and 40°C temperature (Buchi, 2018) for approximately 1 hour. Finally, the extract was dried again in the drier at 40°C for 1 hour (Bimakr et al., 2013) to remove the remaining solvent in the extract.

Preparation of Fatty Acid Methyl Esters (FAME)

Samples were pre-treated to a temperature between 50°C - 60°C and homogenized thoroughly before the testing to obtain the FAME. An aliquot of the sample (100 µL) was mixed with 1mL hexane in a 2mL vial. An aliquot of sodium methoxide (1 µL, 1% w/v) was added to the vial and the mixture was mixed vigorously using a vortex mixer. The mixture was clear at first and then became turbid at the bottom of the solution due to the precipitation of sodium glyceroxide which contains the non-soluble compounds. After a few minutes, the clear upper layer of methyl esters which contains the solubilized fatty acids was pipetted off and can be injected into the gas chromatography (GC) for further analysis (Bimakr et al., 2013).

Gas chromatography Flame Ionization Detector (GC-FID) analysis

Samples were converted to methyl esters which contain the solubilized fatty acids and were injected into the GC for further analysis. The GC analysis was performed using Hewlet-Packard 6890 gas chromatograph, equipped with flame ionization detector (FID) and a BPX70 GC column. Oven temperature was programmed isothermally to 60°C during 0.5 min, and raised to 10°C/min till 180°C for 5 min and then at 5°C/min till 215°C. Then, the temperature was raised to 220°C and finally, the temperature increased to 240°C at 5°C/min and held this temperature for 16 min.

Carrier gas, Helium was used as a carrier gas as the type of column used in this GC will be the capillary column (Alinafiah *et al*., 2021) and its flow rate was 1 mL/min. The injection volume was 1 µL. Standard FAME (Sigma Aldrich, Germany) was used as the authentic sample. The FA determination was accomplished by comparing it with standards and values as percentage of each FA. The determination of FA was performed in triplicate for each sample and expressed as means ± standard deviation.

Experimental designs and statistical analysis

The optimization of the extraction parameters (pressure, temperature and flow rate) for the SFE was done using the Design Expert software. After choosing the ranges of the parameters from previous studies, those values were incorporated into the RSM statistical tool for optimization purposes. Based on Table 1, pressure, temperature and flow rate were chosen as the independent variables and extraction yield was the only response. All the other parameters such as the extraction time (90 min), weight of sample (10 g) and extract collection time (20 hours) were kept constant throughout the experiments.

A three-factor-3-level face-centered design was chosen in the extraction of *B. hispida* seed extract (BHSE), which resulted in a total of 17 runs (Table 2) consisting of 8 factorial points, 6 axial points and 3 center points. For the evaluation of whether the constructed models were adequately fitted with the experimental data, corresponding analysis of variance (ANOVA) was applied using software which functions as numerical optimization for the determination of SFE's optimum conditions.

Results and Discussion

Prediction and optimization using RSM

RSM-central composite design (RSM-CCD) was applied to optimize the SFE conditions of the BHSE. The experimental data obtained according to the model is presented in Table 2. The experimental data was analysed and fitted to linear, interactive (2FI), quadratic and cubic models based on previous studies (Sodeifian et al., 2017). The adequacy of model was tested for response and shown in Table 3.

Table 1: The coded and uncoded values of the independent variables used in the experimental design

Independent Variables	Pressure (Bar)	Temperature (°C)	Flow Rate (g/min)
Coded levels	Level of factor		
+1	100	40	2
0	250	55	6
-1	400	70	10

The result showed that the linear and interactive models had lower R^2, predicted R^2, adjusted R^2 and high F-values compared with the quadratic model which also can be seen in previous studies (Rivas *et al*., 2021; Chalipa et al., 2024; Kumaran et al., 2024). Moreover, the cubic mode was found to be aliased. Therefore, the quadratic model was chosen to describe the current study. Quadratic model has been chosen from most of the published studies related to the optimization using RSM to describe their experimental results (Gan et al., 2020).

Model fitting and statistical analysis

ANOVA was used to indicate which terms are statistically significant and the validity of the experimental models (Abassi *et al*., 2020). Besides the ANOVA result, F-value and corresponding p-values along with the estimated coefficients were presented at Table 3. A higher model which the F-value is 40.85 and the associated lower p-values ($P < 0.0001$) demonstrated that the corresponding coefficients are more significant and illustrate the best fit for both experimental and actual values of the developed model (Peng *et al*., 2019).

In this model, a R^2 value of 0.9813 (very close to 1) shows that there was a good agreement between the experimental and predicted yields of BHSE and the model can reasonably explain the changes of the oil yield under different sets of experimental conditions.

On top of that, the adjusted coefficient of determination (Adjusted $R^2 = 0.9573$) and predicted coefficient of determination (Predicted $R^2 = 0.8567$) were also close to 1 which reflects the result of highly correlated of both experimental and predicted yields and lead to the conclusion that the model had fully fitted the data as agreed by a study (Kothari *et al*., 2021).

The lack of fit was not significant based on the F-value (1.90) and p-value (0.3795) to the pure error. This finding was in line with previous study where the lack of fit was considered as a reference besides R- values and p-values to indicate that the model values provide significance of the regression model to infer the effect of the input variables (Nadeem *et al*., 2021).

A second order polynomial equation was fitted to the experimental data. The constants and coefficients were fitted into the equation 2 below so that the regression equation as a function of independent parameters, namely pressure (A), temperature (B) and flow rate (C) while Y is the oil yield and was obtained as follows (in terms of coded levels):

$$Y = +6.13 - 0.1090A + 0.4620B + 0.9670C + 0.3037AB - 0.1038AC + 0.7987BC - 4.52A2 + 3.76B2 - 4.16C2 \quad (2)$$

In this CCD model, the significance determination for each model was assessed by both p-value and F-value. The influence of the model term on the oil yield was considered significant if the p-value is < 0.05 and larger F-value with small p-value indicates greater significance of the corresponding model item as observed in a study (Louaer *et al*., 2019). According to the result tabulated in Table 3, the linear terms of pressure and temperature showed insignificant impact towards the oil yield while the flow rate showed a significant ($P < 0.05$) impact.

In terms of the interaction terms, interaction terms between temperature and flow rate (BC) were the only terms with significant impact towards the oil yield as agreed previously (Suryawanshi and Mohanty, 2018). Meanwhile, the interaction terms between pressure and temperature (AB) and pressure and flow rate (AC) were not significant.

In a comprehensive analysis of each model item, although the linear terms for the temperature, pressure and flow rate had no significant impact towards the *B. hispida* oil yield, the interaction term of BC and the quadratic terms of those three independent variables ($P < 0.0001$) had significant effects towards the oil yield indicating that these selected variables were also part of the indispensable factors.

Previous studies have found that the quadratic terms of the pressure, temperature and flow rate were significantly interacted, thus proving its effectiveness towards the oil yield (Ishak et al., 2021 as agreed in this study where the three quadratic terms were significantly interacted towards the SFE of BHSE.

Validation of the model was carried out by carrying out SFE using three different sets of parameters which were generated from the design expert software and each of the sets were different from the 17 runs. The result of the validation showed that by using parameters of 70°C, 247 bar and 7 g/min, running in triplicate, result in 8.13% of relative error at 90% confidence interval which was the lowest compared with the other two set of parameters (26.76% & 11.94%). Therefore, the optimised parameter for this model is 70°C, 247 bar and 7 g/min.

Table 2: The experimental designs of CCD and the oil yield measured at different conditions along with the predicted oil yield

		Factor 1	Factor 2	Factor 3	Actual Yield	Predicted Yield
Std. Order	Space Type	A: Pressure (bar)	B: Temperature (°C)	C: Flow Rate (g/min)	Yield (%)	Yield (%)
1	Factorial	100	40	2	0.7	0.8934
2	Factorial	400	40	2	0.01	0.2754
3	Factorial	100	70	2	0.03	0.3876
4	Factorial	400	70	2	0.01	0.2094
5	Factorial	100	40	10	1.66	1.44
6	Factorial	400	40	10	0.01	0.4044
7	Factorial	100	70	10	3.64	3.35
8	Factorial	400	70	10	3.75	3.53
9	Axial	100	55	6	0.99	1.73
10	Axial	400	55	6	2.15	1.51
11	Axial	250	40	6	10.06	9.43
12	Axial	250	70	6	9.63	10.35
13	Axial	250	55	2	1.25	1.01
14	Axial	250	55	10	2.61	2.94
15	Centre	250	55	6	6.36	6.13
16	Centre	250	55	6	6.63	6.13
17	Centre	250	55	6	5.6	6.13

Parameters affecting the response

For the model diagnosis results, the normal distribution of residuals and the comparison between experimental and predicted values showed good linearity which also reflected that the model was capable in expressing the relationship among the selected parameters as shown in Fig. 2 (a) & Fig. 2 (c) (Dao *et al.*, 2019). Fig. 2 (c) shows that the experimental and predicted values were close to the regression line, and it reflects the high R^2 value (0.9813) thus the changes of oil yield can be reasonably explained based on this graph.

Additionally, Fig. 2 (b) shows the normal plot of residuals vs run which indicates that the residuals of the experimental yield were scattered randomly thus, the model is suitable for optimization. The same result can also be found in another study, indicating the appropriateness of the model to suggest the observation of original value is unrelated to the response values (Falowo *et al.*, 2019).

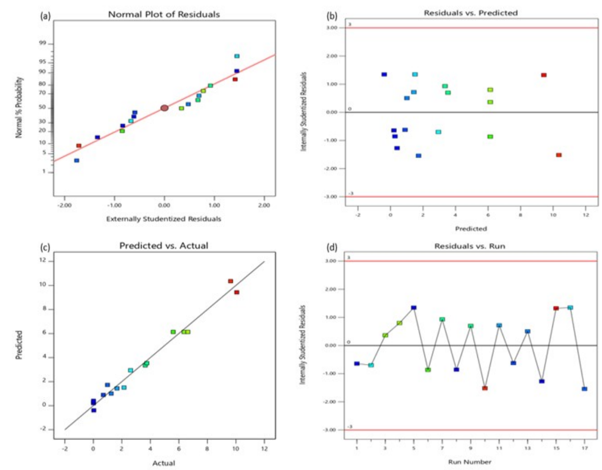

Fig. 2: Statistical analysis of the surface quadratic model

For the determination of large residuals in runs, the standard residuals in the outlier plot should fall into three standard deviations intervals as observed in Fig. 2 (d) and similar results were recorded in previous study (Zhang *et al.*, 2019). Any outlier that exceeds this interval could result in a hidden error in the model or operational error in the experiment (Yingngam *et al.*, 2021).

Table 3: Response surface model adequacy and ANOVA analysis

Source	Std. Dev.	R^2	Adjusted R-square	Predicted R-square	p-value	PRESS
Linear	3.55	0.0660	-0.1495	-0.5031	0.8203	264.12
2FI	3.98	0.0998	-0.4404	-2.6226	0.9432	636.56
Quadratic	0.6848	0.9813	0.9573	0.8567	<0.0001	25.18
Cubic	0.4457	0.9966	0.9819	0.7651	0.1723	41.28

Source	Sum of Squares	df	Mean-square	F-value	p-value
Model	172.44	9	19.16	40.85	< 0.0001
A-Pressure	0.1188	1	0.1188	0.2533	0.6302
B-Temperature	2.13	1	2.13	4.55	0.0703
C-Flow Rate	9.35	1	9.35	19.94	0.0029
AB	0.7381	1	0.7381	1.57	0.2499
AC	0.0861	1	0.0861	0.1836	0.6812
BC	5.10	1	5.10	10.88	0.0131
A^2	54.70	1	54.70	116.63	< 0.0001
B^2	37.81	1	37.81	80.62	< 0.0001
C^2	46.33	1	46.33	98.78	< 0.0001
Residual	3.28	7	0.4690		
Lack of Fit	2.71	5	0.5425	1.90	0.3795
Pure Error	0.5705	2	0.2852		
Cor Total	175.72	16			

Fig. 3 shows the three-dimensional (3D) plots along with their two-dimensional (2D) projections of response surfaces for the graphical representations of regression equation obtained from the RSM analysis. The constant level of the three independent variables (250 bar, 55˚C and 6 g/min) of each operating parameter (pressure, temperature and flow rate) was implemented for the interactive analysis of any of the two parameters through the 3D plots.

Different shapes of the 2D contour plot including elliptical and circular shape can be observed in Fig. 3. Elliptical contour plots mean the interactions between the involved parameters were significant while circular contour plots indicate the interactions were negligible. Previous studies also proved the presence of both shapes providing the visual relationships between response and the experimental levels of each variable and their interactions (Zhai *et al*., 2021). As from my observations, the elliptical contour can be seen at Fig. 3 (c) while Fig. 3 (a) and Fig. 3 (b) produced more circular contour plots.

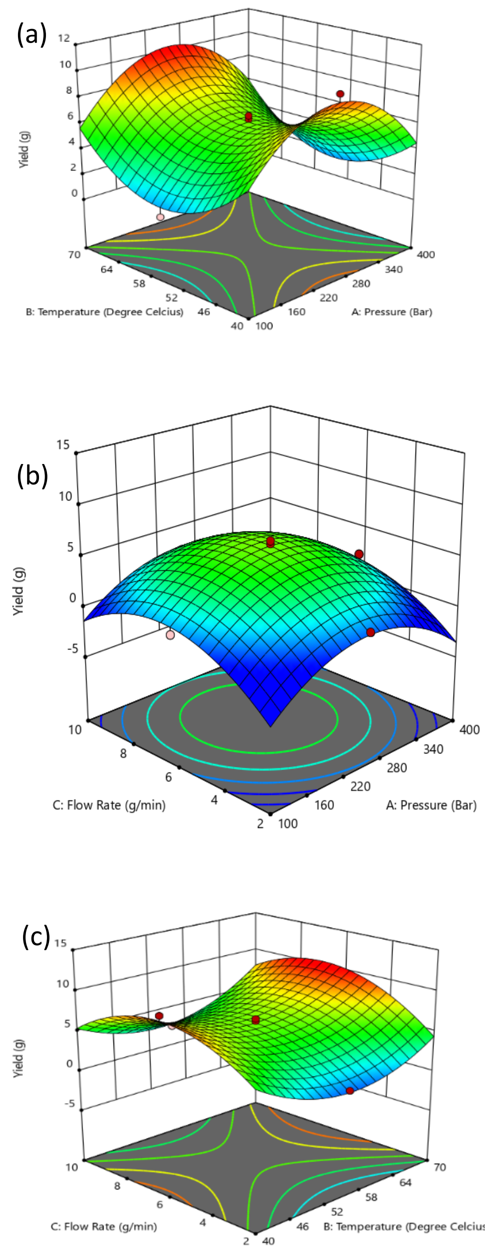

Fig 3: 3D graph and 2D plots show the effects of two-parameter interactions on BHSE

Temperature

As observed in Fig. 3, the impact of temperature was unique as the oil yield increased at both lowest and highest temperature. There are two extraction conditions which affect the impact of temperature towards the oil yield which are the above and below crossover pressure. When there is an increased in temperature, the oil yield increased due to effect of temperature on SC-CO_2 density became less than the vapor pressure at above crossover pressure (Patil et al., 2017). However, below the crossover pressure, the effect of temperature on density supersedes the vapor pressure and at lower temperature, higher SC-CO_2 density contributed to the high solvent power of SC-CO_2 and producing higher oil yield as observed (Nde and Foncha, 2020).

From Table 2, low oil yield was obtained at the lowest temperature (40 ˚C) and pressure (100 bar) As the temperature increased from 40 ˚C to 70 ˚C, the oil yield became reduced at 100 bar and this is because of a reduction of solvation effect to disperse into the sample matrix (Ishak et al., 2021).

Additionally, when there was an increase of pressure from 100 bar to 250 bar at the same temperature (40 ˚C), the oil yield increased due to an increased in SC-CO_2 density and solvation strength (Ishak et al., 2021). However, the significant reduction of oil yield at high temperature (70 ˚C) and pressure (400 bar) decreases the SC-CO_2 density and the contacts between the seed matric and SC-CO_2 thus minimizing the interaction between the solvent and the sample thus lowering the mass transfer during extraction (Suryawanshi and Mohanty, 2018).

In this study, the oil yield was lower as the temperature was reduced as observed in Fig. 4, but as it reached 55˚C, the oil yield started to increase. Similar finding was found, where the oil yield started to be increased from 19.13% to 21.63% when the temperature was increased from 40˚C to 60˚C considering the effect of temperature is ruled by both solvent density and vapor pressure of the oil (Ferrentino *et al*., 2020).

Fig. 3 (c) shows the 3D surface graph of the effects of temperature and flow rate towards the oil yield at fixed pressure (250 bar). The effect of temperature in this study also can be seen at the lowest temperature (40 °C) which produces high oil yield. This research finding is found to be similar with the SFE of chia seed where the oil yield was higher between 40 °C – 45 °C (Ishak *et al*., 2021).

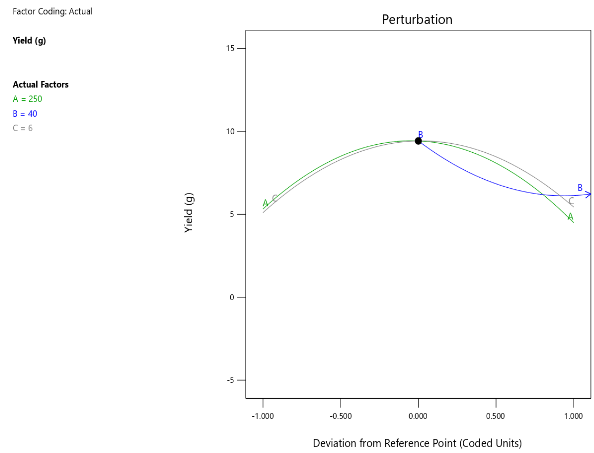

Fig. 4: Effect of individual parameters towards *B hispida* seed oil yield

This situation can also be explained by the positive correlation between yield and extraction temperature when combined with pressure. At 100 bar, the oil yield decreased when the temperature increased, dropping from 0.7% at 40 °C to 0.03% at 70 °C because at critical pressure, oil solubility decreases when the temperature increases, due to the predominant effect of density on solute vapor pressure. Conversely, the oil yield increased from 0.01 at 40 °C to 3.75% at 70 °C because above the critical pressure, the vapor pressure effect dominates, resulting in an increase in solute solubility. The compound's solubility is thus favored or disfavored by increasing the temperature, depending on whether the pressure is lower or higher than the crossover pressure (Allay et al., 2025).

Pressure

Fig. 4 (curve A) shows an increase in pressure at constant flow rate and temperature which did not result in a further increase in the oil yield. The highest yield obtained was at 250 bar, 40 °C and 6 g/min flow rate (10.06%), indicating the minimal impact of pressure towards the oil yield. Nevertheless, the effect of quadratic term of pressure increased significantly at high pressure (greater than 250 bar). The possible reason is that the highly compressed CO_2 led to the reduction in the fluid diffusion coefficient. This counteract effect often resulted in little impact towards the oil yield with high pressure being implemented (Gan *et al*., 2020).

On top of that, the increasing extraction pressure caused a reduction in the solvent diffusivity, hence the convective mass transfer attendant to the extraction process, leading to lower oil recovery (Ahangari *et al*., 2021).

The 3D surface graphs of the effect of pressure and temperature on the yield of *B. hispida* seed at a constant flow rate (C = 6 g/min) are shown at Fig. 3 (a). At the given temperature, the increased in pressure caused the density of the supercritical solvent CO_2 to be higher, which resulted in an increase in the solubility of CO_2 and ultimately increased the oil yield. Higher extraction pressure may result in the elevation of vapor pressure, facilitating the travel of oil onto the surface of the seeds thus improving the oil yield (Peng *et al*., 2019). Thus, the yield of *B. hispida* seed increases significantly with the increase in pressure.

Previous findings have proved the positive impact of the pressure towards the oil yield and their findings were aligned with the current findings where the oil yield increased from 0.99% to 6.36% when the pressure increased from 100 bar to 250 bar. Similarly, the increase of pressure of 200 to 300 bar has resulted in the highest yield of extraction in previous studies (Teixeira *et al*., 2020; Santos et al., 2020). Additionally, the increase of extraction pressure from 100 bar to 169 bar was shown to raise the recovery of sunflower oil from 47.54% to 52.08% (Daraee et al., 2018).

Flow rate of supercritical carbon dioxide

Maximum oil yield can be obtained from the increased fluid flow rate because of the reduction of resistance to mass transfer until the exiting fluid became saturated, consequently, leading to the solute solubility equilibrium (Acevedo-Correa *et al*., 2018). This occurrence can be observed in Fig. 4 (curve C), where the maximum flow rate which resulted in maximum oil yield was at 6 g/min.

In Fig. 3 (c), under the given pressure, the increase in the CO_2 flow could increase the cycle extraction time in the pipeline, thus resulting in an increase of the oil yield. However, as the CO_2 flow bypassed 6 g/min rate, the residence time of CO_2 was too short so the contact time with the extract was reduced which was not suitable to improve the oil yield (Chouaibi *et al*., 2020).

Besides that, the extraction yield of wheat germ oil and raspberry seed oil was the highest at solvent flow rate of 0.4 kg CO_2/h or 6.67g/min (Teslić et al., 2020; Pavlić et al., 2019) which is in-line with the result of the current study because of the increase in concentration gradient and consequently improving the extraction rate.

Identification and Quantitation of Fatty Acid Composition

Table 4 shows the comparison of the FA contents from extracts of both SFE and SE. There were no significant differences in terms of the FA contents for both SE and SFE except for the linoleic acid (LA), myristic acid and oleic acid.

The total content of saturated fatty acid (SFA) (Table 4) was 29.9% from SE and 26.86% from SFE with palmitic acid (13.137 ± 1.077 for SE, 13.32 ± 0.2150 for SFE) accounted to be the highest FA content and these results are also recorded in previous findings (Anwar *et al*., 2011; Bimakr *et al*., 2013). For comparison, the SFAs extracted from the SE were much higher than those extracted using SFE even though they are not statistically significant except for Myristic acid which were statistically significant ($P < 0.05$).

The same result was obtained in previous study (Rosa *et al*., 2019) where the application of different extraction methods can be the reason and lower percentage of PUFAs could contribute to proportional increase in SFA and monounsaturated fatty acid (MUFA) contents (Rosa *et al*., 2019). The amount of SFAs were lower than the unsaturated fatty acids (UFAs) because of the unfavorable high temperature for the extraction of SFAs as observed in Table 4 (Souza *et al*., 2020).

Additionally, the UFAs' extracted using SFE were higher (72.2%) compared to those UFAs extracted using SE (70.5%). These data were agreed by a study (Anwar *et al*., 2011), in which this study used the same type of seed with only differences in the parameters chosen for the extractions. PUFAs were accounted for the highest content of FAs for both types of extractions with PUFAs from SFE were significantly higher than in the SE (P ≤ 0.001) which is similar with previous studies (Rajei *et al*., 2005; Gustinelli *et al*., 2018).

Table 4: Comparison of fatty acids contents between different extraction methods

Fatty Acid Category	Compound Name	Carbon Number	Fatty Acid Composition (%)	
Extraction Type			**SE**	**SFE**
TEC (%)			32.667*** ± 0.333	9.623*** ± 1.688
Saturated Fatty Acids	Octanoic Acid	8:0	0.36 ± 0.032	0.33 ± 0.103
	Decanoic acid	10:0	-	-
	Lauric acid	12:0	0.093 ± 0.009	0.073 ± 0.003
	Tridecanoic acid	13:0	0.207 ± 0.0351	0.56 ± 0.02
	Myristic acid	14:0	1.073* ± 0.078	0.207* ± 0.02
	Pentadecanoic acid	15:0	0.447 ± 0.035	0.247 ± 0.009
	Palmitic acid	16:0	13.367 ± 0.622	13.317 ± 0.124
	Heptadecanoic acid	17:0	0.407 ± 0.007	0.297 ± 0.003
	Stearic acid	18:0	11.36 ± 0.07	10.78 ± 0.103
	Arachidic acid	20:0	1.977 ± 0.02	1.05 ± 0.175
	Behenic acid	22:0	0.587 ± 0.055	-
Total			29.9%	26.86%
Unsaturated Fatty Acids	Myristoleic acid	14:1 n-5	-	-
	Palmitoleic acid	16:1 n-7	0.87 ± 0.017	0.933 ± 0.007
	Elaidic acid trans	18:1	0.497 ± 0.041	-
	Oleic acid	18:1 n-9	5.467**** ± 0.179	2.257**** ± 0.192
	Linoleic acid	18:2 n-6	58.453**** ± 0.423	68.507**** ± 0.151
	Alpha Linoleic acid	18:3 n-3	1.66 ± 0.08	1.44 ± 0.3
	Eicosenoic acid	20:1	1.123 ± 0.019	-
	Erucic acid	22:1 n-9	2.03 ± 0.04	-
Total			70.5%	72.2%

Each value represents the mean ± SEM of triplicate experiments. (*) P ≤ 0.05, (**) P ≤ 0.01, (***) P ≤ 0.001 and (****) P ≤ 0.0001.

The content of the LA and the alpha-linoleic acid (ALA) were analyzed using the optimised parameter from the RSM. Previous findings also showed that majority of the FA content extracted using the SFE was LA and ALA. The parameters affecting the LA and ALA contents are pressure and temperature. Firstly, in terms of the pressure, the change in pressure of a study from 200 bar to 250 bar resulted in an increase of the LA content in raspberry seed oil for 20% and similar trend was observed for the ALA (Campalani *et al*., 2020). This finding was aligned with the result of this current study where the optimised pressure was 247 bar to produce the high yield of the PUFAs.

Besides that, the second parameter which is the temperature, , 70˚C was found to be the best temperature for the extraction of FAs in wild strawberry pomace as well as for the *B. hispida* seed as the application of lower temperature such as 40˚C and 50˚C caused a much lower FA content because of the solubility of solute mainly affected by the increasing vapor tension rather than the CO_2 density reduction (Campalani *et al*., 2020). Also, an increase in temperature from 20˚C to 60 ˚C resulted an increase in LA content for 45% showing the positive impact of the high temperature towards LA (Hernández-Fernández *et al*., 2019).

Conclusion

As a conclusion, based on the CCD model for the optimisation, three parameters were selected and optimised according to the range of values for those parameters. Thus, the set of parameters (70°C, 247 bar and 7g/min) with 8.13% relative error was determined to be the optimised parameter for the BHSE extraction. As for the fatty acid identification, the result shows that the PUFAs were detected mostly in both types of extraction but the BHSE from SFE produced higher PUFAs' content (9.84% differences) and accompanied with advantages of the SFE over the SE especially in terms of its safety towards the operator and the environment because of the solvent recovery and avoidance of the released of harmful solvents to the environment. However, the primary limitation for the SFE is higher operating cost and excessive consumption of energy to convert and maintain the supercritical state of the solvent.

Authors contributions

Conceptualization, H.A.H. and Z.I.S.; methodology, Z.I.S., H.A.H. and R.Z.R.; resources, H.A.H.; writing—original draft preparation, R.Z.R.; writing—review and editing, H.A.H.; supervision, H.A.H. and Z.I.S.; funding acquisition, H.A.H. All authors have read and agreed to the published version of the manuscript.

Acknowledgements

First of all, I would like to express my gratitude for my institution, International Islamic University Malaysia for providing me the platform in completing this project. Furthermore, I would like to thank the postgraduate students from IIUM, for their involvement in the experimental procedures such as research ideas related to the project. Moreover, I would like to express my sincerest appreciation towards the staff in charge for the supercritical fluid extraction equipment from the INHART, IIUM Gombak and to the lecturers and staff from the Department of Pharmaceutical Technology, Kulliyyah of Pharmacy, IIUM Kuantan for their assistance in the experimental procedures. Last but not least, through the support by Fundamental Research Grant Scheme (FRGS19-092-0701), which was received by my main supervisor, the project was successfully completed.

Conflict of interest

The authors report there are no competing interests to declare.

Declaration of generative AI and AI-assisted technologies in the writing process

This manuscript is completed without any usage of AI or AI-assisted technologies during the writing process.

References

Abbasi S., Mirghorayshi M., Zinadini S., Zinatizadeh A. A. (2020). A novel single continuous electrocoagulation process for treatment of licorice processing wastewater: Optimization of operating factors using RSM. *Process Safety and Environmental Protection*, 134, 323-332. DOI: https://doi.org/10.1016/j.psep.2019.12.005

Acevedo-Correa D., Castillo P. M., Martelo R. J. (2018). Effect of the process parameters on the oil extraction yield during supercritical fluid extraction from grape seed. *Contemporary Engineering Sciences*, 11, 611-617. DOI: https://doi.org/10.12988/ces.2018.8250

Ahangari H., King J. W., Ehsani A., Yousefi M. (2021). Supercritical fluid extraction of seed oils – A short review of current trends. *Trends in Food Science & Technology*, 111, 249-260. DOI: https://doi.org/10.1016/j.tifs.2021.02.066

Al Juhaimi F. & Özcan M. M. (2017). Effect of cold press and Soxhlet extraction systems on fatty acid, tocopherol contents, and phenolic compounds of various grape seed oils. *Journal of Food Processing and Preservation*, 1-8. DOI: https://doi.org/10.1111/jfpp.13417

Allay, A., Benkirane, C., Ben Moumen, Fauconnier M.-L., Bouakline H., Nkengurutse J., Caid H. S., Elamrani A., Mansouri F. (2025). Optimizing ethanol-modified supercritical CO_2 extraction for enhanced bioactive compound recovery in hemp seed oil. *Scientific Report* 15, 1-22. DOI: https://doi.org/10.1038/s41598-025-91441-x

Alinafiah S. M., Azlan A., Ismail A., Ab Rashid N.-K. M. (2021). Method development and validation for omega-3 fatty acids (DHA and EPA) in fish using gas chromatography with flame ionization detection (GC-FID). *Molecules*, 26, 1-13. DOI: https://doi.org/10.3390/molecules26216592

Anwar F., Mohammad N. A., Othman F., Saari N. (2011). Inter-varietal variation in the composition of seeds and seed oils from winter melon [*Benincasa hispida* (thunb.) cogn.] fruit. *Pakistan Journal of Botany 43*(4), 2039-2047. https://www.academia.edu/1926348/inter_varietal_variation_in_the_composition_of_seeds_and_seed_oils_from_winter_melon_benincasa_hispida_thunb_cogn_fruit

Bimakr M., Rahman R. A., Taip F. S., Adzahan N. M., Sarker M. Z. I., Ganjloo A. (2013). Supercritical carbon dioxide extraction of seed oil from winter melon (*Benincasa hispida)* and its antioxidant activity and fatty acid composition. *Molecules*, 18, 997-1014. DOI: 10.3390/molecules18010997

Bitwell C., Indra S. S., Luke C., Kakoma M. K. (2023). A review of modern and conventional extraction techniques and their applications for extracting phytochemicals from plants. *Scientific African 19*, 1-19. DOI: https://doi.org/10.1016/j.sciaf.2023.e01585

Boniamin M., Sohag S. U., Ahmad S., Hasan R., Sumi S. Y., Bari Q. I., Dutta S., Mondol M. A. M., Sultana J., Ahmed F. R. S. (2024). Protective effects of nutrients and antioxidant-rich seed oil and sprouted seed oil of *Benincasa hispida* against formaldehyde-induced hepatic and renal damage. *Pharmacological Research - Modern Chinese Medicine 13*, 1-8. DOI: https://doi.org/10.1016/j.prmcm.2024.100555

Buchi. (2018). Rotavapor R-220 Pro Operation Manual. https://assets.fishersci.com/TFS-Assets/CCG/Buchi-Corporation/manuals/R-220_Pro_OM.pdf

Campalani C., Amadio E., Zanini S., Dall'Acqua S., Panozzo M., Ferrari S., De Nadai G., Francescato S., Selva M., Perosa A. (2020). Supercritical CO_2 as a green solvent for the circular economy: Extraction of fatty acids from fruit pomace. *Journal of CO_2 Utilization*, 31, 1-6. DOI: https://doi.org/10.1016/j.jcou.2020.101259

Chalipa Z., Hosseinzadeh M., Nikoo M. R. (2024). Performance evaluation of a new sponge-based moving bed biofilm reactor for the removal of pharmaceutical pollutants from real wastewater. *Scientific Reports 14*, 1-16. DOI: https://doi.org/10.1038/s41598-024-64442-5

Chouaibi M., Rigane K., Ferrari G. (2020). Extraction of Citrullus colocynthis L. seed oil by supercritical carbon dioxide process using response surface methodology (RSM) and artificial neural network (ANN) approaches. *Industrial Crops & Products*, 158, 1-15. DOI: https://doi.org/10.1016/j.indcrop.2020.113002

Dao T. P., Nguyen D. C., Tran T. H., Thinh P. V., Hieu V. Q., Nguyen D. V. V., Nguyen T. D., Bach L. G. (2019). Modeling and optimization of the orange leaves oil extraction process by microwave-assisted hydro-distillation: The response surface method based on the central composite approach (RSM-CCD model). *Journal of Chemistry*, 12,2, 666-676. DOI: http://dx.doi.org/10.31788/RJC.2019.1225107

Daraee A., Ghoreishi S. M., Hedayati A. (2018). Supercritical CO_2 extraction of chlorogenic acid from sunflower (*Helianthus annuus*) seed kernels: Modeling and optimization by response surface methodology. *The Journal of Supercritical Fluids*, 1-35. DOI: https://doi.org/10.1016/j.supflu.2018.10.001

Falowo O. A., Oloko-Oba I. M., Betiku E. (2019). Biodiesel production intensification via microwave irradiation-assisted transesterification of oil blend using nanoparticles from elephant-ear tree pod husk as a base heterogeneous catalyst. *Chemical Engineering and Technology*, 1-46. DOI: https://doi.org/10.1016/j.cep.2019.04.010

Ferrentino G., Giampiccolo S., Morozova K., Haman N., Spilimbergo S., Scampicchio M.

(2020). Supercritical fluid extraction of oils from apple seeds: Process optimization, chemical characterization, and comparison with a conventional solvent extraction. *Innovative Food Science and Emerging Technologies*, 1-37. DOI: https://doi.org/10.1016/j.ifset.2020.102428

Gade S. R., Meghwal M., Prabhakar P. K. (2020). Engineering properties of dried ash gourd (*Benincasa hispida* Cogn) seeds: Mass modelling and its analysis. *Journal of Food Process Engineering*, e13545, 1-16. DOI: 10.1111/jfpe.13545

Gan Y., Xu D., Zhang J., Wang Z., Wang S., Guo H., Zhang K., Li Y., Wang Y. (2020). Rana chensinensis ovum oil based on CO_2 supercritical fluid extraction: Response surface methodology optimization and unsaturated fatty acid ingredient analysis. *Molecules*, 25, 1-14. DOI: 10.3390/molecules25184170

Gustinelli G., Eliasson L., Svelander C., Andlid T., Lundin L., Ahrn´e L., Alminger M. (2018). Supercritical fluid extraction of berry seeds: Chemical composition and antioxidant activity. *Journal of Food Quality*, 1-10. DOI: https://doi.org/10.1155/2018/6046074

Hernández-Fernández M. A., Rojas-Avilla A., Vazquez-Landaverde P. A., Cornejo-Mazón M., Dávilla-Ortiz G. (2019). Volatile compounds and fatty acids in oleoresins from *Vanilla Planifolia Andrews* obtained by extraction with supercritical carbon dioxide. *CyTA Journal of Food*, 1, 419-430. DOI: https://doi.org/10.1080/19476337.2019.1593247

Hou N.-C., Gao H.-H., Qiu Z.-J., Deng Y.-H., Zhang Y.-T., Yang Z.-C., Gu L.-B., Liu H.-M., Zhu X.-L., Qin Z., Wang X.-D. (2024). Quality and active constituents of safflower seed oil: A comparison of cold pressing, hot pressing, Soxhlet extraction and subcritical fluid extraction. *LWT Food Science and Technology*, *200*, 1-10. DOI: https://doi.org/10.1016/j.lwt.2024.116184

Ishak I., Hussain N., Coorey R., Abd Ghani M. (2021). Optimization and characterization of chia seed (*Salvia hispanica L.*) oil extraction using supercritical carbon dioxide. *Journal of CO_2 Utilization*, 45, 1-14. DOI: https://doi.org/10.1016/j.jcou.2020.101430

Kothari R., Ahmad S., Samykano M., Tyagi V. V., Pandey A. K., Saidur R. (2021). Optimization of extraction process of jatropha oil by using quenching agent. *IOP Conference Series Materials Science and Engineering*, 1127, 1-8. DOI: 10.1088/1757-899X/1127/1/012003

Kumaran P., Sengodan N., Kumar S., Anderson A., Prakash S. (2024). Investigating the emissions and performance of ethanol and biodiesel blends on Al2O3 thermal barrier coated piston engine using response surface methodology design - multiparametric optimization. *Environmental Research and Technology* *7*(3), 406-421. DOI: https://10.35208/ert.1443393

Louaer M., Zermane A., Larkeche O., Meniai A.-H. (2019). Experimental study and optimization of the extraction of Algerian date stones oil (*Phoenix dactylifera L.*) using supercritical carbon dioxide. *Journal of Food Process Engineering*, 1-9. DOI: 10.1111/jfpe.13049

Mazurek B., Ryzko U., Kostrzewa D., Chmiel M., Kondracka M. (2022). Brief characteristics of oxidative stability, fatty acids and metal content in selected berry seed extracts obtained by the SFE technique and used as potential source of nutrients. *Food Chemistry*, 367, 1-10. DOI: https://doi.org/10.1016/j.foodchem.2021.130752

Megashree B. M., Shantha T. R., Venkateshwarlu G., Bhat S. (2017). Comparative pharmacognostical and histochemical studies on *Benincasa Hispida* (Thunb.)

CogN.– Fruit and seed. *International Journal of Herbal Medicine*, 5(4): 17-24. https://www.florajournal.com/archives/?year=2017&vol=5&issue=4&part=A&ArticleId=404

Mondal I. H., Rangan L., Uppaluri R. V. S. (2020). Process-product characteristics of tray-dried *Benincasa hispida*. *Journal of Food Process and Preservation*, 1-13. DOI: 10.1111/jfpp.14697

Muzahid A. A., Sharmin S., Hossain S., Ahamed K. U., Ahmed N., Yeasmin S., Ahmed N. U., Saha B. K., Rana M., Maitra B., Bhuiyan N. H. (2023). Analysis of bioactive compounds present in different crude extracts of *Benincasa hispida* and *Cucurbita moschata* seeds by gas chromatography-mass spectrometry. *Heliyon 9*, 1-9. DOI: https://doi.org/10.1016/j.heliyon.2022.e12702

Nadeem F., Bhatti I. A., Ashar A., Yousaf M., Iqbal M., Mohsin M., Nisar J., Tamam N., Alwadai N. (2021). Eco-benign biodiesel production from waste cooking oil using eggshell derived MM-CaO catalyst and condition optimization using RSM approach. *Arabian Journal of Chemistry*, 14, 1-11. DOI: https://doi.org/10.1016/j.arabjc.2021.103263

Nawaz H., Shad M. A., Rehman N., Andaleeb H., Ullah N. (2020). Effect of solvent polarity on extraction yield and antioxidant properties of phytochemicals from bean (*Phaseolus vulgaris*) seeds. *Brazilian Journal of Pharmaceutical Sciences*, 1-9. DOI: http://dx.doi.org/10.1590/s2175-97902019000417129

Patil P. D., Dandamudi K. P. R., Wang J., Deng Q., Deng S. (2017). Extraction of bio-oils from algae with supercritical carbon dioxide and co-solvents. *Journal of Supercritical Fluids*, 1-36. DOI: https://doi.org/10.1016/j.supflu.2017.12.019

Pavlić B., Pezo L., Marić B., Peić L., Zeković Z., Solarov M. B., Teslić N. (2019). Supercritical fluid extraction of raspberry seed oil: Experiments and modelling. *The Journal of Supercritical Fluids*, 1-41. DOI: https://doi.org/10.1016/j.supflu.2019.104687

Peng L. W., Mohd-Nasir H., Mohd Setapar S. H., Ahmad A., Lokhat D. (2019). Optimization of process variables using response surface methodology for tocopherol extraction from Roselle seed oil by supercritical carbon dioxide. *Industrial Crops & Products*, 1-11. DOI: https://doi.org/10.1016/j.indcrop.2019.111886

Peng Y., Khaled U., Alrashed A. A.A.A., Meer R., Goodarzi M., Sarafaz M.M. (2019). Potential application of Response Surface Methodology (RSM) for the prediction and optimization of thermal conductivity of aqueous CuO (II) nanofluid: A statistical approach and experimental validation. *Physica A*, 1-23. DOI: https://doi.org/10.1016/j.physa.2020.124353.

Rajei A., Barzegar M., Yamini Y. (2005). Supercritical fluid extraction of tea seed oil and its comparison with solvent extraction. *European Food Research and Technology*, 220, 401-405. DOI: 10.1007/s00217-004-1061-8

Rivas M. A., Casquete R., Cordoba M. d. G., Benito M. J., Hernandez A., Ruiz-Mayano S., Martin A. (2021). LWT – *Food Science and Technology*, 145, 1-7. DOI: https://doi.org/10.1016/j.lwt.2021.111305

Rosa A., Era B., Masala C., Nieddu M., Scano P., Fais A., Porcedda S., Piras A. (2019). Supercritical CO_2 extraction of waste citrus seeds: Chemical composition, nutritional and biological properties of edible fixed oils. *European Journal of Lipid Science and Technology*, 1-33. DOI: 10.1002/ejlt.201800502

Santos O. V., Lorenzo N. D., Souza A. L. G., Costa C. E. F., Conceição L. R. V., Lannes S. C. d. S., Teixeira-Costa B. E. (2020). CO_2 supercritical fluid extraction of pulp and nut oils from *Terminalia* catappa fruits: Thermogravimetric behaviour, spectroscopic and fatty acid profiles. *Food Research International*, 1-7. DOI: https://doi.org/10.1016/j.foodres.2020.109814

Shakya A., Chaudhary S. K., Bhat H. R., Ghosh S. K. (2020). Acute and sub-chronic toxicity studies of *Benincasa hispida* (Thunb.) cogniaux fruit extract in rodents. *Regulatory Toxicology and Pharmacology*, 118;1-9. DOI: https://doi.org/10.1016/j.yrtph.2020.104785

Sodeifian G., Sajadian S. A., Ardestani N. S. (2017). Experimental optimization and mathematical modelling of the supercritical fluid extraction of essential oil from *Eryngium billardieri*: Application of simulated annealing (SA) algorithm. *The Journal of Supercritical Fluids*, 127, 146-157. DOI: http://dx.doi.org/10.1016/j.supflu.2017.04.007

Souza R. d. C. d., Machado B. A. S., Barreto G. d. A., Leal I. L., Anjos J. P. d., Umsza-Guez M. A. (2020). Effect of experimental parameters on the extraction of grape seed oil obtained by low pressure and supercritical fluid extraction. *Molecules*, 25, 1-27. DOI: 10.3390/molecules25071634

Suryawanshi B. & Mohanty B. (2018). Modelling and optimization: Supercritical CO_2 extraction of *Pongamia pinnata* (L.) seed oil. *Journal of Environmental Chemical Engineering*, 1-39. DOI: https://doi.org/10.1016/j.jece.2018.04.014

Teixeira G. L., Maciel L. G., Mazzutti S., Gonçalves B. C., Ferreira S. R. S., Block J. M. (2020). Composition, thermal behavior and antioxidant activity of pracaxi *(Pentaclethra macroloba)* seed oil obtained by supercritical CO_2. *Biocatalysis and Agricultural Biotechnology*, 1-42. DOI: https://doi.org/10.1016/j.bcab.2020.101521

Teslić N., Bojanić N., Čolović D., Fišteš A., Rakić D., Solarov M. D., Zeković Z., Pavlić B. (2020). Conventional versus novel extraction techniques for wheat germ oil recovery: multi-response optimization of supercritical fluid extraction. *Separation Science and Technology*, 1-16. DOI: https://doi.org/10.1080/01496395.2020.1784941

Yingngam B., Brantner A., Treichler M., Brugger N., Navabhatra A., Nakonrat P. (2021). Optimization of the eco-friendly solvent-free microwave extraction of *Limnophila aromatica* essential oil. *Industrial Crops & Products*, 165, 1-16. DOI: https://doi.org/10.1016/j.indcrop.2021.113443

Zhang Y., Niu S., Lu C., Gong Z., Hu X. (2019). Catalytic performance of NaAlO2/γ-Al2O3 as heterogeneous nanocatalyst for biodiesel production: Optimization using response surface methodology. *Energy Conversion and Management*, 1-11. DOI: https://doi.org/10.1016/j.enconman.2019.112263

Zhai X., Xiang Y., Tian Y., Wang A., Li Z., Wang W., Hou H. (2021). Extraction and characterization of cellulose nanocrystals from cotton fiber by enzymatic hydrolysis-assisted high-pressure homogenization. *Journal of Vinyl & Additive Technology*, 1-14. DOI: 10.1002/vnl.21849uwiishak

Zakharenko A., Romanchenko D., Thinh P. D., Pikula K., Hang C. T. T., Yuan W., Xia X., Chaika V., Chernyshev V., Zakharenko S., Razgonova M., Chung G., Golokhvast K. (2020). Features and advantages of supercritical CO_2 extraction of sea cucumber *Cucumaria frondose japonica Semper*, 1868. *Molecules*, 25, 1-9. DOI: 10.3390/molecule